Surface Changes and Role of Buried Water Molecules during the Sulfane Sulfur Transfer in Rhodanese from *Azotobacter vinelandii*: A Fluorescence Quenching and Nuclear Magnetic Relaxation Dispersion Spectroscopic Study†

Mauro Fasano,*,‡ Maria Orsale,§ Sonia Melino,§ Eleonora Nicolai,||,⊥ Fabio Forlani,@ Nicola Rosato,||,⊥ Daniel Cicero,§,⊥ Silvia Pagani,@ and Maurizio Paci§,⊥

Dipartimento di Biologia Strutturale e Funzionale, University of Insubria, via Jean H. Dunant 3, 21100 Varese, Italy, Dipartimento di Scienze e Tecnologie Chimiche, University of Rome "Tor Vergata", Via della Ricerca Scientifica, 00133 Rome, Italy, Dipartimento di Scienze Biochimiche, University of Rome "Tor Vergata", Via della Ricerca Scientifica, 00133 Rome, Italy, Dipartimento di Scienze Molecolari Agroalimentari, University of Milano, Via Celoria 2, 20133 Milano, Italy, and Istituto Nazionale Fisica della Materia, Sez. B. of Rome, Italy

Received December 10, 2002; Revised Manuscript Received May 20, 2003

ABSTRACT: The *Azotobacter vinelandii* rhodanese is a sulfurtransferase enzyme that catalyzes the transfer of the outer sulfur atom from thiosulfate to cyanide. Recently, investigations by NMR relaxation on the ^{15}N-enriched protein reported that interdomain contacts are rigidly maintained upon the sulfane sulfur transfer from the enzyme to the substrate. The modality of the enzymatic mechanism is then confined to a surface interaction, including dynamics of water molecules buried in the tertiary structure. Thus, investigations have been carried out by fluorescence, circular dichroism, and nuclear magnetic relaxation dispersion measurements. The comparison of circular dichroism spectra of the persulfurated enzyme and the sulfur-free form indicated that small changes occur. Fluorescence quenching studies have been performed to evaluate the conformational changes during catalysis using the fluorescent probe 8-anilinonaphthalene-2-sulfonic acid, and acrylamide, iodide, and cesium ions as quenchers. Changes in exchange dynamics of water molecules buried in the structure with bulk water, observed by nuclear magnetic relaxation dispersion, are due to local conformational transitions, likely involving residues around the active site, and are consistent with the global correlation time found by ^{15}N relaxation. These results, taken together, provide important information for elucidating the conformational features of the mechanism of action of the enzyme either in the role of a selective donor of a sulfur atom to small-sized substrates (i.e., to cyanide, transforming it into thiocyanate) or in the role of sulfur insertase for the formation of the Fe_2S_2 iron−sulfur cluster in sulfur-deprived ferredoxins.

Sulfurtransferase enzymes are widely distributed among plants, animals, and bacteria. In vitro, these enzymes catalyze the transfer of the outer sulfur atom from thiosulfate to cyanide, this atom being converted to a persulfide or properly a "sulfane" (*1*−*3*). During the catalytic process, the enzyme cycles between two intermediates, the free enzyme (E)[1] and the sulfur-loaded enzyme (ES). Although they are widely distributed, the physiological role of the sulfurtransferase enzymes has not been established. Previous works demonstrated that mammalian rhodanese (thiosulfate:cyanide sulfurtransferase, EC 2.8.1.1) can act as a sulfur insertase, and regenerate redox centers in Fe−S proteins (*4*, *5*).

Rhodanese from *Azotobacter vinelandii* (RhdA) is the only thiosulfate-cyanide sulfurtransferase identified and characterized so far in the nitrogen-fixing bacteria (*6*). The gene *rhdA* encoding the enzyme has been identified, cloned, and overexpressed in *Escherichia coli* (*7*). The three-dimensional structure has been recently elucidated (*8*), resembling that of bovine (*Bos taurus*) rhodanese (*9*). Structural studies of these proteins have shown that they consist of a single polypeptide chain arranged in two domains linked by a connecting loop. The conformation of the main chain about the active site is highly similar in RhdA with respect to bovine rhodanese, although some residues in the active site are different. The level of amino acid sequence identity for these two enzymes is ∼22%.

Each domain displays an α/β topology, with a central parallel five-stranded β-sheet surrounded by α-helices on both sides. Keim et al. (*10*) proposed that this structure arose from the gene duplication of an ancestral single-domain enzyme, after divergent evolution of the two proteins and a fusion event. The catalytic functional site of rhodanese is

† This research was partly supported by grants "Solfotransferasi procariotiche" (1999−2001), MIUR-PRIN (2002−2003), CNR Target Oriented Project "Biotecnologie", and CNR Coordinated Project.

* To whom correspondence should be addressed. Telephone: +390331339450. Fax: +390331339459. E-mail: mauro.fasano@uninsubria.it.

‡ University of Insubria.

§ Dipartimento di Scienze e Tecnologie Chimiche, University of Rome "Tor Vergata".

|| Dipartimento di Scienze Biochimiche, University of Rome "Tor Vergata".

⊥ Istituto Nazionale Fisica della Materia.

@ University of Milano.

[1] Abbreviations: 2,8-ANS, 8-anilinonaphthalene-2-sulfonic acid; E, sulfur-free rhodanese; ES, sulfur-loaded rhodanese; IPTG, isopropyl β-D-thiogalactopyranoside; NMRD, nuclear magnetic relaxation dispersion; RhdA, *A. vinelandii* rhodanese.

10.1021/bi0273359 CCC: $25.00
Published on Web 06/26/2003

located close to a cleft between the two domains; all side chains essential for the catalysis are provided by only the second domain.

In the past, proton relaxation data (measured at a proton Larmor frequency of 26 MHz) and ^{35}Cl NMR relaxation data have been reported for bovine rhodanese (*11*, *12*), and a tightening of the binding site cleft, interpreted as a reduction of the accessibility of water, was suggested on the basis of a decrease in T_1 for the ES and E forms of the enzyme. Indeed, the protein surface may act as a source of water relaxation, and a different exposure to protein surface might affect the relaxation behavior of the bulk water protons. However, single-frequency relaxation measurements cannot distinguish between relaxivity contributions due to surface-bound water and those from water molecules buried within the protein core and able to exchange on the NMR time scale (*13*).

In this paper, circular dichroism (CD), nuclear magnetic relaxation dispersion (NMRD), and fluorescence spectroscopy measurements have been taken in an effort to investigate the structural modality of the enzymatic mechanism. The comparison of results reported for the sulfur-loaded (ES) and sulfur-free (E) forms, i.e., after the transfer of the sulfur atom to the substrate, led us to conclude that local conformational transition(s) due to side chain rearrangements are involved in the catalytic mechanism observed in vitro and that these changes do affect the exchange dynamics of water molecules buried in the three-dimensional structure with bulk water. These results are in very good agreement with the results independently obtained by ^{15}N relaxation NMR experiments on the isotopically uniformly enriched protein, which clearly indicated that no large backbone conformational transition occurs during the enzymatic cycle, excluding therefore a large rearrangement of the interdomain contacts. These results have been summarized here and will be reported in detail elsewhere (paper in preparation).

MATERIALS AND METHODS

Rhodanese Preparation. The protein was expressed in *E. coli* strain BL21 pREP4 using the pQER1 plasmid, downstream from the six-histidine tag coding region. Antibiotics for the selection of *E. coli* transformants were used at the following concentrations: 100 μg/mL ampicillin and 25 μg/mL kanamycin. Overexpression of the recombinant protein was induced by addition of IPTG to a midlog culture. RhdA was purified by chromatography on a Ni−NTA agarose column (Qiagen) (*7*). The His-tagged protein was eluted by addition of 200 mM imidazole and precipitated in 75% saturated ammonium sulfate. The protein concentration was determined using an A_{280} of 1.3 for a 0.1% solution (*14*) and a molecular mass of 31 kDa. Rhodanese activity was measured by the discontinuous colorimetric assay described by Sörbo (*15*). The presence of the His tag did not affect enzymatic activity. The E form was prepared by adding a 10-fold molar excess of cyanide to ES rhodanese in 50 mM Tris-HCl buffer and 0.3 M NaCl (pH 7.4) followed by a 10 min incubation at 303 K.

Fluorescence Quenching Measurements. Steady-state fluorescence measurements have been carried out with a ISS-K2 fluorometer (ISS, Champaign, IL) equipped with an external bath circulator to maintain the temperature at 293 K; the protein concentration was kept constant at 6 μM. Spectra were taken over the wavelength range of 290−440 nm ($\Delta\lambda = \pm 2$ nm) with an excitation wavelength of 280 ± 2 nm. 2,8-ANS binding was studied by measuring the fluorescence emission spectra (from 450 to 550 nm, $\Delta\lambda = \pm 1$ nm) of the probe using an excitation wavelength of 350 ± 1 nm. The protein concentration used in these fluorescence measurements was 3 μM. The fluorescence intensity was expressed by the Stern−Volmer equation (*16*):

$$F_0/F = 1 + k_q\tau_0[Q] = 1 + K_{sv}[Q] \quad (1)$$

where F_0 and F are the fluorescence intensities in the absence and presence of the quencher, Q, respectively, k_q is the bimolecular quenching constant, τ_0 is the lifetime of the fluorophore in the absence of the quencher, [Q] is the concentration of the quencher, and K_{sv} ($=k_q\tau_0$) is the Stern−Volmer quenching constant.

The steady-state fluorescence anisotropy is defined by

$$\langle r\rangle = \frac{I_V - GI_H}{I_V + 2GI_H} \quad (2)$$

where I_V and I_H are the intensity of the vertically and horizontally polarized components, respectively, of the fluorescence excited by vertically polarized light and G is the ratio of the sensitivity of the detection system for vertically and horizontally polarized light.

The measurements were carried out by inserting two Glan-Thompson polarizers on the excitation and emission pathways.

Circular Dichroism. CD spectra were measured with a Jasco 600 CD spectropolarimeter calibrated with camphorsulfonic acid. Spectra were recorded between 200 and 250 nm using a path length of 0.1 cm, a time constant of 1.0 s, a 2 nm bandwidth, and a scan rate of 2 nm/min. A total of four scans was used for each experiment. The average was corrected by four scans of the solvent alone. A 0.1 cm sealed and thermostatically controlled quartz cell was used for all CD spectra. The mean residue ellipticity (θ_{MRW} in degrees per square centimeter per decimole) is reported. The samples for circular dichroism experiments were prepared at a RhdA concentration of 5 μM in 20 mM Tris-HCl buffer (pH 7.4). The sulfur-free form was obtained by incubation of the sulfur-loaded enzyme with 50 μM KCN for 20 min at 303 K.

Nuclear Magnetic Relaxation Dispersion (NMRD). NMRD profiles, i.e., plots of solvent water proton relaxation rates as a function of the applied magnetic field, were measured on a Stelar Spinmaster FFC field cycling spectrometer (Stelar, Mede, Italy), operating in a field range from 1.85×10^{-4} to 0.47 T (proton Larmor frequencies from 8 kHz to 20 MHz). A volume of ~0.5 mL of the protein solution (0.49 and 0.44 mM for the E and ES forms, respectively) was placed in a 10 mm outside diameter glass tube. The temperature was set and maintained at 278 K by using a built-in temperature controller equipped with a liquid nitrogen evaporator and directly measured in the probehead with a mercury thermometer. All solutions were allowed to equilibrate for 15 min before each measurement. Measurements recorded over a period of 24 h did not show a time

dependence of the results, thus excluding the occurrence of slower processes. The relaxometer is able to switch the magnetic field strength on a millisecond time scale and works under complete computer control. As a blank, the measurement of T_1 of the buffer [20 mM Tris-HCl (pH 7.4)] was performed at the same temperature. The uncertainty associated with $1/T_1$ measurements is reported in Figure 6 by means of error bars and is always less than 1%, on average. NMRD profiles have been analyzed in terms of a simple Lorentzian dispersion (*13*, *17*), as described by the following equation:

$$R_1 = R_0(T) + Y_0 + (A\tau_c)/(1 + 3\omega^2\tau_c^2) \qquad (3)$$

where $R_0(T)$ is the relaxation rate of the blank (i.e., the buffer) solution at a given temperature T, Y_0 is the part of R_1 that remains in the extreme motional narrowing regime (i.e., the nondispersive contribution), A is the mean square fluctuation of the lattice variable coupled to the observed nuclear spin, and τ_c is the correlation time for the time-dependent spin−lattice coupling. The term $3\omega^2\tau_c^2$ takes into account both single- and double-quantum coherence relaxation pathways.

The hydration shell of the protein mainly contributes to the nondispersive part of the NMRD profile, since the residence time of these water molecules is shorter than the protein reorientational time. By assuming that the dispersive part of the NMRD profile is determined by water molecules buried within the protein core and still able to exchange with bulk water in the NMR time scale, τ_c turns out to be the reorientational correlation time of the protein, and the amplitude parameter A would be related to the number of internal water molecules (N_I) as described hereafter.

$$N_I S_I^2 = AN_T/\omega_D^2 \qquad (4)$$

where N_T is the number of total water molecules (per protein) and ω_D is the intramolecular dipole frequency. In the case of hydrogen nuclei, $\omega_D = 2.36 \times 10^5$ rad/s (*13*). S_I is the mean-square generalized order parameter for the internal water molecules and cannot be greater than 1 (*13*).

RESULTS AND DISCUSSION

Fluorescence Spectroscopy. Fluorescence experiments were performed either to quantitatively evaluate the effect of sulfur transfer on the intrinsic fluorescence of the enzyme or to study the effects of reagents such as 8-anilinonaphthalene-2-sulfonic acid (2,8-ANS), potassium iodide, cesium chloride, and acrylamide on the fluorescence of tryptophan residues in RhdA.

Intrinsic fluorescence emission of tryptophan residues in a protein provides a sensitive probe of structural properties of the protein microenvironment. Quenching agents act through collision with the excited fluorophore in such a way that a change in quenching properties is reflective of a change in the accessibility of the quenching agent. The intrinsic fluorescence of RhdA is due to seven tryptophan and ten tyrosine residues. The fluorescence quenching of the rhodanese has been used, in the past, to monitor the state of the enzyme during the sulfurtransferase activity. The quantum yield of rhodanese intrinsic fluorescence is higher with the enzyme in the sulfur-free (E) form rather than in the sulfur-loaded (ES) form (*18*); this finding might be explained either in terms of a long-range energy transfer (*19*) or a conformational change in the protein structure (*20*). The modifications toward persulfuration of the active site cysteine of RhdA are accompanied by a quenching of the intrinsic protein fluorescence as shown by the decreasing values of relative quantum yield × 100, calculated by integration of fluorescence spectra and reported in Table 1. A 4 nm shift of the fluorescence spectrum of the ES form toward the E form has been observed, indicating an increased average exposure of tryptophan(s) to the solvent in the E form (Table 1). Measurements of fluorescence anisotropy are widely utilized in biochemical research as estimations of rotational correlation times of proteins and local motion of tryptophan residues. Therefore, as we can see in Table 1, we have different values of anisotropy (indicated with the symbol $\langle r \rangle$; see eq 2) for the two forms. As the tertiary structures of the two forms are similar, the different anisotropy values measured here are due to different local Trp mobility and/or different average fluorescence lifetimes between the two forms (Table 1).

Table 1: Parameter Values Obtained from Fluorescence Spectroscopy

enzyme	relative quantum yield (×100)[a]	center of mass (nm)[b]	anisotropy $\langle r \rangle$
ES	55	336 ± 1	0.139 ± 0.003
E	100	340 ± 1	0.112 ± 0.003

[a] Calculated by integration of fluorescence spectra. [b] Center of mass of fluorescence spectra.

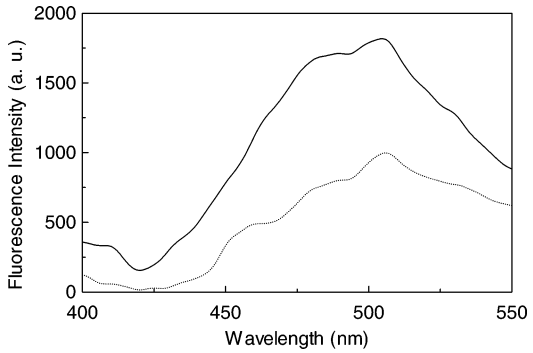

FIGURE 1: Intensity of the fluorescence spectrum of 2,8-ANS, added to both forms of the protein at a final concentration ratio of 60:1 (180 μM 2,8-ANS and 3 μM RhdA): 2,8-ANS added to the ES form (···) and 2,8-ANS added to the E form (—).

Furthermore, we have studied the interaction of the two forms of the RhdA protein with the apolar fluorescence probe 2,8-ANS, which increases its fluorescence quantum yield upon noncovalent binding to hydrophobic regions of proteins (*16*, *22*). 2,8-ANS was added to both forms of protein at a final concentration ratio of 60:1 (180 μM 2,8-ANS and 3 μM RhdA). Figure 1 shows spectra of 2,8-ANS in the presence of ES and E forms of RhdA. When the enzyme is in the E form, the fluorescence intensity of 2,8-ANS, measured at 475 nm, increased ~2 times compared to that of the ES form (Figure 1). The 2,8-ANS binding studies support the presence of apolar sites on rhodanese that display different accessibilities to the 2,8-ANS molecules in the ES and E forms, in a manner consistent with a model that includes an accessibility change coupled with the catalytic activity.

Iodide and cesium ions are large polar anions and cations, respectively, with access to fluorophores (tryptophan resi-

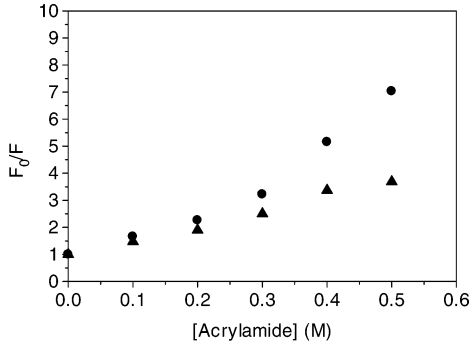

FIGURE 2: Fluorescence quenching of RhdA with increasing concentrations of acrylamide. Data for E are represented with circles and data for ES with triangles.

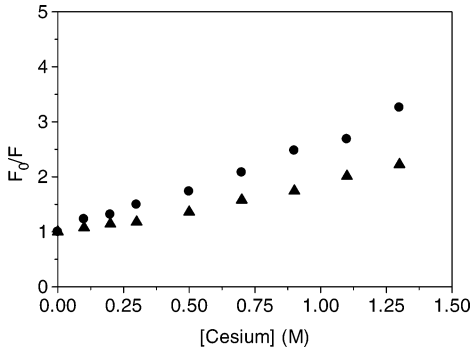

FIGURE 3: Fluorescence quenching of RhdA with increasing concentrations of cesium chloride. Data for E are represented with circles and data for ES with triangles.

dues) of the protein more exposed to the solvent, whereas acrylamide is a polar nonionic quencher and can penetrate into the protein. Relative quenching effects were analyzed by Stern−Volmer plots, as described in Materials and Methods; according to eq 1, the ratio of intrinsic fluorescence intensity in the presence and absence of the quencher is expected to show a linear dependence upon the concentration of the quencher. In these plots, more effective quenching is reflected by a greater slope of the plot.

The results of quenching studies using acrylamide are displayed in Figure 2. The effects may be related to an increase in the level of exposure of hydrophobic patches on the protein surface in the E form compared to that in the ES form. Therefore, acrylamide is slightly more effective in quenching the fluorescence of the E form than the ES form. This is consistent with the above-reported results indicating that tryptophan residues are less solvent-exposed in the ES form than in the E form. As reported in Figure 2 for the ES form, a linear Stern−Volmer plot indicates the presence of a single class of fluorophores that are all equally accessible to the quencher. On the other hand, the Stern−Volmer plot for the E form deviates from linearity. This nonlinearity can be described by a kinetic model that assumes two parallel processes, one represented by bound and the second by free quencher molecules (*16*).

Figures 3 and 4 report Stern−Volmer plots for polar ionic quenchers, i.e., cesium chloride and potassium iodide, respectively. Iodide, being negatively charged and hydrated as well, is likely to quench only surface tryptophan residues, and its effectiveness is apparently dependent upon the neighboring charge environment (*21*). In these experiments, a nonlinear behavior was observed for both E and ES forms,

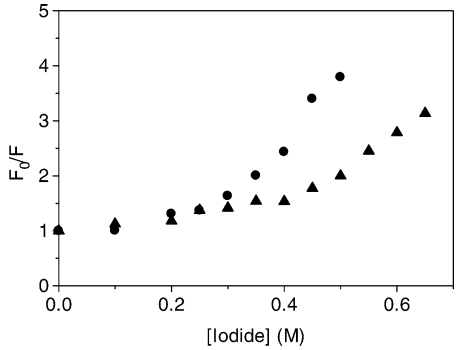

FIGURE 4: Fluorescence quenching of RhdA with increasing concentrations of potassium iodide. Data for E are represented with circles and data for ES with triangles.

indicating the presence of at least two parallel quenching processes (*22*).

Cesium ion was the least effective of the three quenchers used in this study. The effect of cesium chloride as a cationic quencher is shown in Figure 3. For both RhdA catalytic states, a linear Stern−Volmer plot is observed, although the quenching is more effective for the E form. Iodide ions have more evident effects than cesium ions at low concentrations, thus suggesting that the tryptophans are more shielded from cationic quenchers than anionic ones, perhaps by the presence nearby of positively charged side chains. Accordingly, the crystallographic structure of RhdA shows that the interdomain region is rich of basic residues (*8*).

Fluorescence data reported here show that interconversion of ES and E catalytic states of RhdA is correlated to differential binding of fluorescence quenchers, indicating a larger accessibility to the solvent of the latter form and indicating that a local conformational change of side chains is involved during the catalytic cycle. In the previous fluorescence studies on the double mutant of bovine rhodanese, in which either Cys254 or Cys263 was substituted with a Ser residue (C254/263S), the removal of the extra sulfur resulted in a conformation of the rhodanese with increased solvent accessibility to tryptophan residues and increased hydrophobic exposure (*23*). The cysteine residues at positions 254 and 263 are located within the α-helix after the catalytic loop; in particular, the substitution of Cys254 and the removal of the transferable sulfur atom generated enough structural flexibility in the active site region. In our case, RhdA has only the catalytic cysteine residue (see above), Gly237 and Leu246 being the residues corresponding to positions 254 and 263 in the bovine rhodanese, respectively. Like the E form of the double mutant C254/263S, the sulfur-free form of RhdA shows a nonlinear Stern−Volmer plot in the fluorescence quenching by acrylamide. Structural flexibility in the active site region accounts for the major accessibility of the E form of the double mutant. In particular, substitution of Cys with Ser in α-helix D′ (or helix 11) caused a destabilizing effect only after ES to E conversion (*23*). Hence, the assembly of the side chains of RhdA around the active site should be more flexible and more accessible to the ions and hydrophobic quencher than the wild type of the bovine enzyme.

Circular Dichroism Spectroscopy. Far-UV CD measurements of the two forms of the enzyme were performed under the same condition as the fluorescence measurements reported above. The spectral profile of RhdA in the ES form

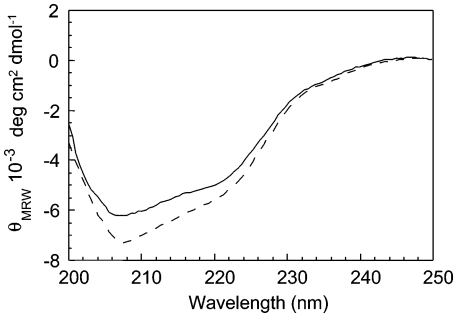

FIGURE 5: Far-UV CD spectra of RhdA [6 μM in 50 mM Tris-HCl (pH 7.2)] in the ES form (—) and E form (– – –).

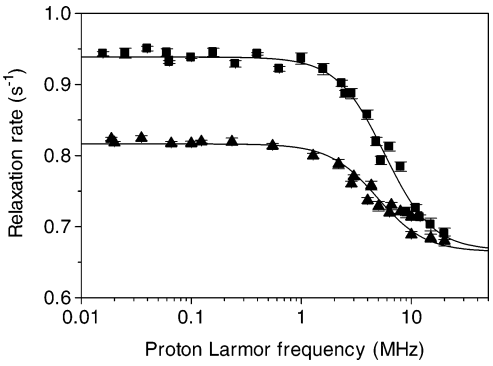

FIGURE 6: Nuclear magnetic relaxation dispersion (NMRD) profiles of RhdA in the ES form (●) and the E form (▲) in 20 mM Tris-HCl buffer, at 275 K and pH 7.2. The experimental points are reported with experimental error bars. The solid lines indicate the fitting obtained according to eq 3. For further details, see the text.

is roughly comparable to that of the enzyme in the sulfur-free form (E) (Figure 5). The E form has a greater overall ellipticity, and its 208 nm/222 nm ratio is different in the two spectra. This indicates that very limited conformational changes in the two structural domains of the protein occur upon going from the ES form to the sulfur-free form (E) of the enzyme.

Nuclear Magnetic Relaxation Dispersion (NMRD). NMRD is a powerful technique for investigating structural and dynamic aspects of protein solutions. In the case of diamagnetic proteins, the interaction of water with the tertiary and quaternary structure of the protein determines the relaxation properties of the solvent. Therefore, the analysis of water relaxation provides a picture of protein dynamics as a distribution of motion frequencies able to cause relaxation (*13*, *17*, *24*−*28*). To gain a more detailed picture of the water−protein interaction in both catalytic states of RhdA, NMRD profiles have been determined. Figure 6 reports the NMRD profile of the enzyme in the ES and E forms. For dilute protein solutions, the frequency dependence of the solvent water relaxation rate is almost Lorentzian, as expected for freely rotating noninteracting spherical proteins. In other cases, the shape of the NMRD profile deviates from ideality, and a stretched relaxation dispersion is observed (*26*). Profiles reported in Figure 6 show a standard Lorentzian behavior, and analysis by the model-free approach did not improve significantly the quality of the fitting. The analysis of the profiles using eq 3 affords the parameter set reported in Table 2. As can be noticed, transfer of sulfur from Cys230 of ES to cyanide does not affect the molecular correlation time τ_c. The value of 18.0 ns is in perfect agreement with the mean value observed from NMR relaxation properties of the uniformly ^{15}N-enriched protein (manuscript in preparation).

Table 2: Parameter Values Obtained by Fitting the ^{1}H Relaxation Dispersion Data in Figure 6 to eq 3[a]

enzyme	Y_0 (s^{-1})	A ($\times 10^{-6}$ s^{-2})	τ_c (ns)
E	0.01 ± 0.002	8.0 ± 0.1	18.0 ± 0.2
ES	0.01 ± 0.002	13.6 ± 0.2	18.0 ± 0.3

[a] The concentrations of the enzyme are 0.49 and 0.44 mM for the E and ES forms, respectively.

The higher value of the amplitude parameter (i.e., A values in Table 2) observed for the ES state suggests a larger number of protein-bound water molecules in the intermediate−fast exchange regime than in the E state. Indeed, A values provide quantitative information about the number of water molecules contributing to the overall NMRD effect (see eq 4). By assuming that the amplitude value of 8.0 × 10^6 s^{-2} reported in Table 2 for the E form is entirely due to buried water molecules, we should expect that 16 water molecules are buried within the E conformation and that all of them are able to exchange with bulk water in an amount of time longer than the reorientational correlation time (*13*). On the other hand, NMRD parameters reported in Table 2 indicate an amplitude value of 13.6 × 10^6 s^{-2} for the ES form, consistent with at least 30 water molecules having a residence time longer than the reorientational correlation time. Therefore, half of the localized water molecules become fast-exchangeable on the NMR time scale upon going from the ES to the E form. In this situation, labile water molecules no longer contribute to the amplitude of the profile, since their relaxation rate is faster than their exchange rate. However, ^{1}H NMRD data cannot discriminate between buried water molecules and internal labile hydrogens, and the amplitude data should be treated with some caution because the high-frequency plateau is not accurately defined, like in this case. An analysis of the same time scale by means of ^{17}O relaxation dispersion would definitely be of great help (*13*). Nevertheless, the highest protein concentration that can be investigated in a stable form (about 0.5 mM) is too low to permit this kind of approach.

Nondispersive terms (Y_0 in Table 2) are due to the hydration shell of the protein and therefore proportional to the molecular surface. They are consistent with a 31 kDa protein (*13*, *28*), since a recent systematic analysis of a number of different proteins suggests a similar value for a protein of this size (*13*, *28*). Thus, the marked changes observed in the NMRD profiles in terms of the amplitude parameter A should be related to a different contribution from inner hydration water molecules, in terms of their number and lifetime. Considering the very limited changes revealed from CD experiments reported above, one can argue that the conformation of the protein in the catalytic state E is very similar with respect to the ES form and that the observed changes should result from different exchange dynamics of localized hydration water molecules and/or labile protein hydrogens with bulk water protons, providing a rather different source of magnetic relaxation.

The molecular structure around the active site of the ES form of RhdA [PDB entry 1E0C (*8*)] shows that a small conformation change of some of the residues around the active site Cys230 may occur upon going from the E to ES state. In fact, the decrease in the intrinsic fluorescence and

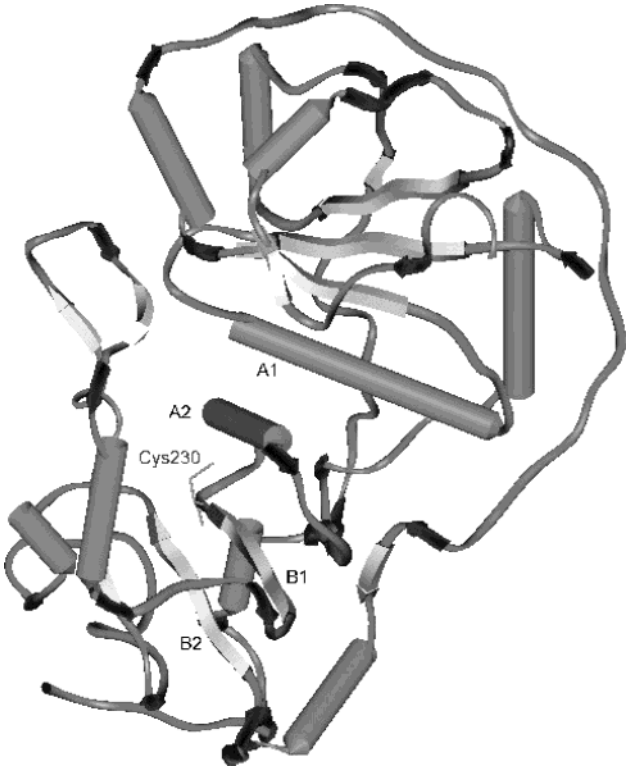

FIGURE 7: Three-dimensional structural representation of *A. vinelandii* rhodanese [PDB entry 1E0C (*8*)]. Cylinders represent α-helices, arrows β-sheets, and coils turns. A1 and A2 correspond to the helices of residues 93−105 and 211−217, respectively, and B1 and B2 correspond to the β-strands of residues 225−229 and 251−254, respectively; the catalytic Cys230 residue is shown with sticks.

the NMRD profiles indicate that some changes occur around the charged loop reported in Figure 7. On the other hand, inspection of the interface between subunits, obtained from crystal data of the ES form [PDB entry 1E0C (*8*)], indicates that relevant interdomain interactions are present around the active site (residues 220−247), between the side chains of the helix made up of residues 93−105 (A1), belonging to the first structural domain, and in the β-strands (B1 which is residues 225−229 and B2 which is residues 251−254) in front of one another. Likely, very small local conformational changes in the active site loop (residues 220−247) upon going from the ES to E state are indicated by CD spectroscopy and thus could determine different accessibility to protons of buried water molecules. The invariance of the correlation time τ_c, on the other hand, indicates that conformational changes involving the whole tertiary structure do not occur.

It is relevant to observe that the results of a parallel study on the uniformly isotopically ^{15}N-labeled protein led to independently obtained results in complete agreement with those reported here. These results will be here briefly summarized. To further characterize the possible differences between the two states of RhdA, ^{15}N T_1 and T_2 relaxation times as well as steady-state ^{1}H−^{15}N NOEs have been measured. The ^{1}H−^{15}N correlation experiments (not shown) have been carried out with uniformly labeled samples of RhdA in the two forms (ES and E). These results will be reported in detail elsewhere. One form could be readily converted into the other by adding potassium cyanide or thiosulfate and then dialyzing out the excess of the reagent. Both spectra show a remarkable dispersion of chemical shift and line shape characteristics, indicating a stable fold of the protein in both forms. The position of catalytic Cys230 has been unequivocally assigned in the two spectra by comparison with the chemical shift obtained with a selectively labeled sample (paper in preparation). A closer inspection of the position of the peaks in the two spectra reveals a high degree of similarity. Only few peaks (six of 250) show a $\delta > 0.1$ ppm, one of which is that for Cys230 ($\delta = 0.19$ ppm), and other 15 exhibit δ values between 0.1 and 0.5 ppm. This observation indicates only slight changes in the backbone conformation of RhdA when converting the E form into the ES form. However, a different situation has been observed in the case when RhdA was first treated with sodium thiosulfate, and then without dialysis being carried out, an excess of potassium cyanide was added to produce the E form.

As expected from the high degree of similarity of the observed chemical shifts, one can argue that, also in the absence of the backbone sequential assignment, data obtained in the two cases were similar. The observed average values were as follows: $\langle T_1 \rangle = 1.54$ s, and $\langle T_2 \rangle = 40.6$ ms. Using the T_1/T_2 ratio approach, it was possible to calculate a correlation time of 16.8 ns. When the temperature at which these measurements were performed (20 °C) was taken into account, this value is reasonable for a monomeric form of the enzyme (molecular mass of 31.0 kDa). In accordance with the high level of dispersion of observed chemical shifts, most of the residues of RhdA show no significant contribution of internal motions in the relaxation parameters of ^{15}N, as can be deduced from the fact that only 18 of 242 peaks exhibited an ^{1}H−^{15}N NOE <0.6 (not shown). Very similar results were observed for the E form (data not shown). The measured values in the latter case were as follows: $\langle T_1 \rangle = 1.50$ s, and $\langle T_2 \rangle = 40.2$ ms (yielding the same overall correlation time). This result indicates that there is no significant change in the overall conformation of the molecule, and the global shape of the enzyme in the two forms remains almost unchanged.

As can be readily observed, no significant difference was detected, showing that the relative absence of internal motion of most of these peaks, and as a consequence of the active site as a whole, remains unaltered in the two conformations. Those independently obtained results will be reported in detail elsewhere, but overall, they further indicate that removal of the sulfur from the ES form of RhdA produces little change in the overall conformation of the enzyme. No significant differences were observed in the backbone conformation and in the flexibility between the two forms, and the global correlation time, obtained from ^{15}N NMR relaxation of the two forms of the protein, remains unchanged.

In conclusion, results of this study indicate that the conformation of the enzyme in the ES and E form appears to be similar, thus safely excluding a large conformational change with a rearrangement of interdomain contacts, and the differences are only due to a small number of residues. A conformational change is likely to occur for the side chains around the active site. In fact, the results reported here from fluorescence quenchers indicate that a variety of side chains interact differently in the two states of the enzyme depending on the chemical nature of the quenchers. As shown in Figure

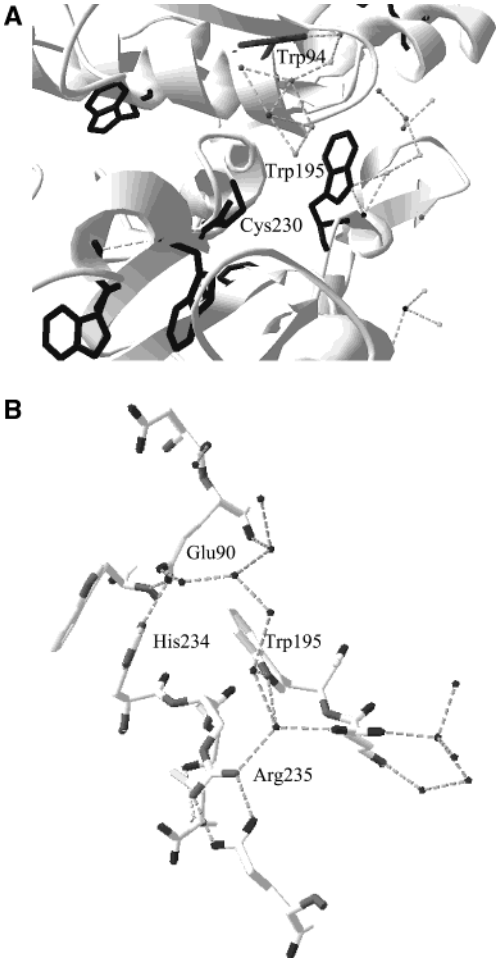

FIGURE 8: Detailed view of the active site of *A. vinelandii* rhodanese [PDB entry 1E0C (*8*)]. (A) Location of the tryptophan residues around the catalytic cysteine. Trp94 and Trp195 are shown to interact with water clusters. (B) Polar residues around Trp195 participate in the stabilization of an extended water network at the opening of the active site.

8A, Trp195 acts as a gate at the entrance of the active site, and interacts with a network of hydrogen-bonded water molecules. It appears therefore likely that a conformational change in this region will affect both water mobility and Trp accessibility. Mobile side chains involving interactions with localized water molecules (see Figure 8B) give the conformational flexibility suitable for operating the recognition mechanism before the action of the enzyme. This feature is probably necessary for its role in sulfur insertase, i.e., for the formation of the Fe_2S_2 iron−sulfur cluster as in sulfur-deprived ferredoxins (*29*). In fact, it appears to be obvious that this latter role requires a quite rigid scaffold and a complex interaction pattern involving a rather large number of recognition events, probably electrostatic, on the molecular surface. In this case, the role of the buried water molecule would be extremely important both by being interposed in the binding and by being a modulator of the release process after the enzymatic action. Proteins with a single rhodanese domain such as the senescence-associated protein Sen1 from *Arabidopsis thaliana* (*30*), the sulfide dehydrogenase from *Wolinella succinogenes* (*31*), and the single-domain GlpE from *E. coli* (*32*, *33*), which recently has been characterized and structurally elucidated, would provide help in understanding these structural changes during the catalytic cycle and their role in the physiological substrate selectivity. Further studies using the selective isotope labeling of the RhdA protein are underway, and the results can give further insights into the details of the role of structural and dynamic features of the active site in the enzymatic mechanism. As a whole, results obtained here should highlight the potential role that NMRD can assume in the investigation of the role of surface conformational changes of diamagnetic proteins, in particular, regarding the release of buried water molecules during biological action.

ACKNOWLEDGMENT

We thank the anonymous referee whose critical suggestions contributed to the improvement of the paper in the definition of the role of buried water.

REFERENCES

1. Westley, J. (1980) Rhodanese and the sulfane pool, in *The Enzymatic Basis of Detoxification* (Jakoby, W. B., Ed.) Vol. 2, pp 245−261, Academic Press, New York.
2. Ray, W. K., Zeng, G., Potters, M. B., Mansuri, A. M., and Larson, T. J. (2000) *J. Bacteriol. 182*, 2277−2284.
3. Beinert, H. (2000) *Eur. J. Biochem. 267*, 5657−5664.
4. Finazzi Agrò, A., Mavelli, I., Cannella, C., and Federici, G. (1976) *Biochem. Biophys. Res. Commun. 68*, 553−560.
5. Pagani, S., Eldridge, M., and Eady, R. R. (1987) *Biochem. J. 244*, 485−488.
6. Pagani, S., Franchi, E., Colnaghi, R., and Kennedy, C. (1991) *FEBS Lett. 278*, 151−154.
7. Colnaghi, R., Pagani, S., Kennedy, C., and Drummond, M. (1996) *Eur. J. Biochem. 236*, 240−248.
8. Bordo, D., Deriu, D., Colnaghi, R., Carpen, A., Pagani, S., and Bolognesi, M. (2000) *J. Mol. Biol. 298*, 691−704.
9. Ploegman, J. H., Drent, G., Kalk, K. H., Hol, W. G., Heinrikson, R. L., Keim, P., Weng, L., and Russell, J. (1978) *Nature 273*, 124−129.
10. Keim, P., Heinrikson, R. L., and Fitch, W. M. (1981) *J. Mol. Biol. 151*, 179−197.
11. Blicharska, B., Koloczek, H., and Wasylewski, Z. (1982) *Biochim. Biophys. Acta 708*, 326−329.
12. Man, M., and Bryant, R. G. (1974) *J. Biol. Chem. 249*, 1109−1112.
13. Halle, B., Denisov, V. P., and Venu, K. (1999) in *Biological Magnetic Resonance* (Krishna, N. R., and Berliner, L. J., Eds.) Vol. 17, pp 419−484, Kluwer Academic/Plenum Publishers, New York.
14. Pagani, S., Sessa, G., Sessa, F., and Colnaghi, R. (1993) *Mol. Biol. Int. 29*, 595−604.
15. Sörbo, B. (1953) *Acta Chem. Scand. 7*, 1137−1145.
16. Lakowicz, J. R. (1983) *Principles of Fluorescence Spectroscopy*, p 260, Plenum Publishing Corp., New York.
17. Koenig, S. H., and Brown, R. D. (1990) *Prog. Nucl. Magn. Reson. Spectrosc. 22*, 487−567.
18. Davidson, B., and Westley, J. (1965) *J. Biol. Chem. 241*, 5168−5176.
19. Finazzi-Agrò, A., Federici, G., Giovagnoli, C., Cannella, C., and Cavallini, D. (1972) *Eur. J. Biochem. 28*, 89−93.
20. Chow, S. F., Horowitz, P. M., Westley, J., and Jarabak, R. (1985) *J. Biol. Chem. 260*, 2763−2770.
21. Eftink, M. R., and Ghiron, C. A. (1981) *Anal. Biochem. 114*, 199−227.
22. Somogyi, B., Szarka, A., and Lakos, Z. (1995) *Biochem. Biophys. Res. Commun. 209*, 936−943.
23. Islam, T. A., Miller-Martini, D. M., and Horowitz, P. M. (1994) *J. Biol. Chem. 269*, 7908−7913.
24. Hallenga, K., and Koenig, S. H. (1976) *Biochemistry 15*, 4255−4263.
25. Bryant, R. G. (1996) *Annu. Rev. Biophys. Biomol. Struct. 25*, 29−53.
26. Halle, B., Johannesson, H., and Venu, K. (1998) *J. Magn. Reson. 135*, 1−13.
27. Kiihne, S., and Bryant, R. G. (2000) *Biophys. J. 78*, 2163−2169.
28. Bryant, R. G. (1996) *Annu. Rev. Biophys. Biomol. Struct. 25*, 29−53.

29. Halle, B., Johannesson, H., and Venu, K. (1998) *J. Magn. Reson. 135*, 1−13.
30. Kiihne, S., and Bryant, R. G. (2000) *Biophys. J. 78*, 2163−2169.
31. Bertini, I., Fragai, M., Luchinat, C., and Parigi, G. (2000) *Magn. Reson. Chem. 38*, 543−550.
32. Pagani, S., Bonomi, F., and Cerletti, P. (1984) *Eur. J. Biochem. 142*, 361−366.
33. Oh, S. A., Lee, S. Y., Chung, I. K., Lee, C. H., and Nam, H. G. (1996) *Plant Mol. Biol. 30*, 739−754.
34. Krafft, T., Gross, R., and Kroger, A. (1995) *Eur. J. Biochem. 230*, 601−606.
35. Ray, W. K., Zeng, G., Potters, M. B., Mansuri, A. M., and Larson, T. J. (2000) *J. Bacteriol. 182*, 2277−2284.
36. Bordo, D., Larson, T. J., Donahue, J. L., Spallarossa, A., and Bolognesi, M. (2000) *Acta Crystallogr. A56*, 1691−1693.

BI0273359